

Three-dimensional mixture theory simulations of turbulent flow over dynamic rippled beds

A. M. Penko & J. Calantoni

Marine Geosciences Division, Naval Research Laboratory, USA

Abstract

The highly turbulent, sediment-laden flow above rippled beds in the wave bottom boundary layer (WBBL) is poorly understood and difficult to quantify mainly because of our failure to understand the fundamental interaction forces driving sediment transport. However, recent advances in high performance computing allow for highly resolved simulations of fluid-sediment dynamics in the WBBL to examine the small-scale fluctuations of boundary layer processes and characterize seabed morphology. A three-dimensional mixture theory model, SedMix3D, solves the unfiltered Navier-Stokes equations for the fluid-sediment mixture with an additional equation describing sediment flux. Mixture theory treats the fluid-sediment mixture as a single continuum with effective properties parameterizing the intra- and inter-phase interactions with closure relations for the mixture viscosity, diffusion, hindered settling, and particle pressure. We validate results obtained with SedMix3D using temporally and spatially resolved fluid velocity measurements acquired with a particle image velocimetry (PIV) system in a free-surface laboratory flume. Measured two-dimensional velocity fields are compared to two-dimensional vertical slices from the three-dimensional simulation domain. We examine the hydrodynamics of the flow by comparing bulk flow statistics, and swirling strength. In general, results from SedMix3D were in excellent agreement with the observations. We believe SedMix3D captures the essential physics governing two-phase turbulent flow over ripples for the conditions represented by the experiments and should provide us with a powerful research tool for studying the dynamics of seafloor bedforms.

Keywords: ripples, bedforms, numerical modeling, turbulence, multiphase flow, mixture theory, model-data comparison.



1 Introduction

Despite advances in computing and laboratory observational technology, there still exist many unknowns about the small-scale interactions driving two-phase hydrodynamics in the seafloor boundary layer. Past work has extensively studied the flow structure over static (or fixed) sand beds [1–5]. These studies have broadened our knowledge on vorticity dynamics of oscillatory flow over ripples; however, they lack the dynamic coupling between the fluid and sediment, which influences turbulence production/dissipation and resulting bed morphology. Because strong correlations exist between the sediment transport, near bed fluid velocity, and bed morphology, coupling these processes will be necessary to accurately model bottom boundary layer flow and the resulting sediment entrainment/deposition.

A three-dimensional numerical model solving the unfiltered Navier-Stokes equations using mixture theory is presented here. Mixture theory treats the fluid-sediment mixture as a continuum with the inter- and intra-phase interactions parameterized with closure relations. The model is validated quantitatively through comparisons of time-dependent and spatially varying velocities as well as bulk flow statistics measured under scaled laboratory conditions.

2 Experimental set-up

The observations were made in a wave flume at the Fluid Mechanics Laboratory at Delft University of Technology, Netherlands using a particle image velocimetry technique [6]. The wave flume is 42 m in length, 0.8 m in width, and 1 m in height, with the bottom covered with a layer of sediment. A material typically used for sand blasting was chosen for the sediment with a mean grain diameter of 0.054 cm and a specific gravity of 1.2. A Dantec particle image velocimeter (PIV) system consisting of a 120 mJ Nd-Yag pulsed laser synchronized with a 1 MegaPixel camera was used to capture two-dimensional vertical (x - z) plane optical images. The sampling window (11 cm \times 11 cm) was located approximately 29 m from the wave generator in a water depth of about 0.31 m. For this experiment, the wave generator produced regular waves 5 cm in height with a period of 2 s.

The laser was placed in a watertight housing located approximately 27 cm above the bed and the camera was placed outside the flume. An Acoustic Doppler Velocimeter (ADV) time-synchronized with the PIV system measured the free-stream velocity approximately 17 cm above the bed. The camera captured image pairs (10 ms time lag between pair members) of the sampling window for 60 s bursts at approximately 12 Hz. Suspended sediment, organic matter, and micro-bubbles acted as seeding agents in the water column. The velocity vectors were calculated by correlating the image pairs using 64×32 pixel interrogation windows with 50% overlap. The resulting spatial resolution of the vector field was 3.48 mm \times 1.74 mm. Outliers were removed with a three standard deviation filter and replaced with the local ensemble average.



3 Methodology

SedMix3D solves the unfiltered Navier-Stokes equations with an additional sediment flux equation for a fluid-sediment mixture resulting in the time-dependent sediment concentration and three-component velocity vector field [7]. The model treats the fluid-sediment mixture as a single continuum with effective properties that parameterize the fluid-sediment and sediment-sediment interactions including a bulk hindered settling velocity, a shear-induced diffusion, an effective viscosity, and a particle pressure. The sediment flux equation models the concentration of sediment by describing the balance between advection, sedimentation due to gravity, and shear-induced diffusion. Grid spacing was on the order of a sediment grain diameter and time step was $O(10^{-5} \text{ s})$. The model only simulates flow in the boundary layer (i.e., no free surface). The numerical scheme is finite difference with second-order central differences employed on a staggered grid. The boundary conditions for the velocities and concentration are periodic in the horizontal. At the top of the domain, the u velocity is assumed to follow the free-stream while the v and w velocities are set to zero. A no-slip condition exists for the velocities at the bottom boundary (i.e., deep inside the sand bed). The initial concentration is equal to the concentration of a fully packed bed at the bottom boundary ($\phi = 0.63$) and zero at the top boundary.

The modeling framework of SedMix3D includes governing equations for sediment flux, mixture continuity, and mixture momentum. The mixture continuity equation was derived by combining the fluid and sediment phase continuity equations,

$$\frac{\partial \rho}{\partial t} + \nabla \cdot (\rho \mathbf{u}) = 0, \quad (1)$$

where \mathbf{u} is the mixture velocity and ρ is the mixture density,

$$\rho = \phi \rho_s + (1 - \phi) \rho_f, \quad (2)$$

where ϕ is the sediment volumetric concentration, and ρ_s and ρ_f are the sediment and fluid densities, respectively. The mixture momentum equation was derived from the sum of the individual phase momentum equations,

$$\rho \frac{\partial \mathbf{u}}{\partial t} + \rho \mathbf{u} \cdot \nabla \mathbf{u} = -\nabla P + \nabla \cdot (\mu \nabla \mathbf{u}) + \mathbf{F} - \rho \mathbf{g}, \quad (3)$$

where P is the mixture pressure, μ is the effective viscosity, \mathbf{F} is the external driving force vector per unit volume, and \mathbf{g} is gravitational acceleration (981 cm s^{-2}). SedMix3D employs a modified Eilers [8] equation to represent effective viscosity, μ , here scaled by the pure water viscosity, μ_f

$$\frac{\mu}{\mu_f} = \left[1 + \frac{0.5[\mu]\phi}{1 - \phi/\phi_m} \right]^2, \quad (4)$$



where $[\mu]$ is the intrinsic viscosity, a dimensionless parameter representing the sediment grain shape, and $0.0 < \phi < 0.63$, where the lower bound represents pure water and upper bound roughly corresponds to the maximum concentration of unconsolidated sediment. Here, we fix the maximum value of the effective viscosity by specifying $\phi_m = 0.66$. The intrinsic viscosity parameter, $[\mu]$, was 2.5 to represent spherical particles [9].

The concentration of sediment is modeled with a sediment flux equation [10] that balances the temporal gradients in sediment concentration with advection, gravity, and shear-induced diffusion,

$$\frac{\partial \phi}{\partial t} + \mathbf{u} \cdot \nabla \phi = D \nabla^2 \phi - \frac{\partial \phi W_t}{\partial z}, \quad (5)$$

where W_t is the concentration specific settling rate,

$$W_t = W_{t0} (1 - \phi)^q, \quad (6)$$

where W_{t0} is the settling rate of a single particle in a clear fluid and q is an empirical constant [11]. The shear-induced diffusion of sediment, D , is a function of grain size, volumetric concentration, and mixture stresses [12].

4 Results

The model forcing was derived from the free stream velocity measured by the ADV in the experiment (Fig. 1). The first four wave periods were considered model spin-up periods. All quantities used in the following comparisons were calculated after discarding the four model spin-up periods. Flow quantities were

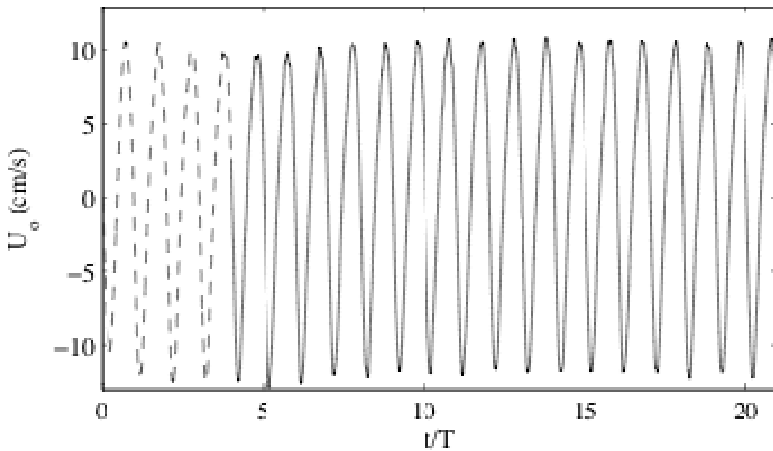


Figure 1: Free-stream velocity recorded by the ADV in the experiment (solid lines) and the four model spin-up periods (dashed lines).

time- and ensemble-averaged over a total of 17 wave periods. We compared a two-dimensional velocity field (x - z plane) from the simulation to the two-dimensional velocity field extracted from the PIV measurements. The simulated x - z plane chosen for comparison here resulted from the minimization of the temporal RMS deviation of the horizontal and vertical velocity RMS deviation. Here we examine the difference between the simulated and observed mean and standard deviation of the horizontal velocity and the ensemble-averaged swirling strength.

4.1 Horizontal velocity mean and standard deviation

The simulated and observed horizontal mean flow profiles at varying locations over the bed are plotted in fig. 2. The maximum difference between the simulated and observed mean flow is less than 2 cm/s at all locations along the ripples. The simulated mean flow agrees very well with the observations over the peaks of the ripples (e.g., $x = 3$ cm, 7 cm, and 8.5 cm), matching the maximum, minimum, and shape of the mean horizontal velocity profile. In the first and last

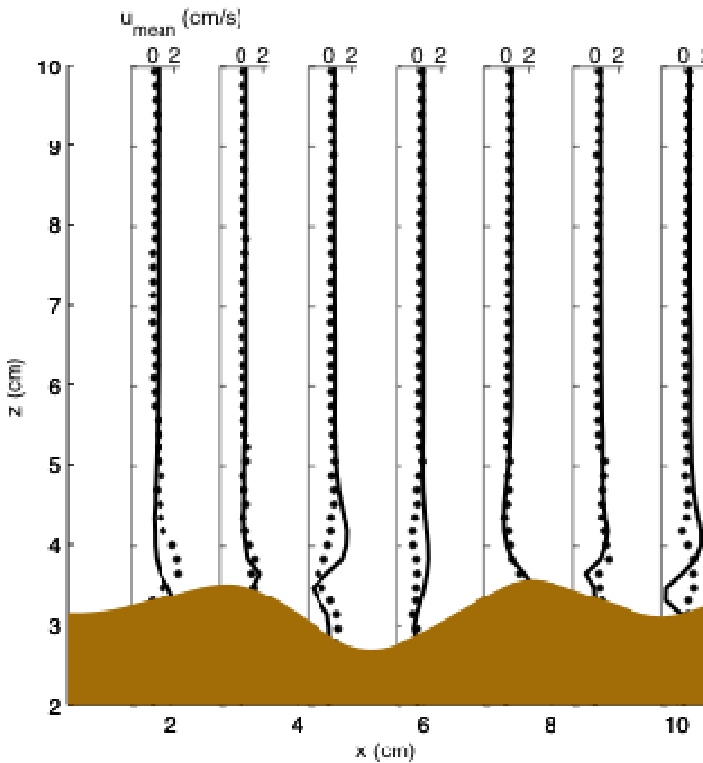


Figure 2: Mean horizontal velocity profiles from the simulation (lines) and observations (dots) at varying locations above the bed.

profiles ($x = 1.5$ and 9.8 cm), there is about a 2 cm/s difference between the simulated and observed horizontal maximum and minimum mean velocity. Fig. 3 is a plot of the standard deviation of the horizontal velocity at the same locations as fig. 2. Contrary to the mean flow, there is better agreement between the simulated and observed standard deviation of the velocity in the troughs of the ripples. In the troughs, the simulated and observed standard deviations are within 2 cm/s. The model overestimates the standard deviation above the crests of the ripples by a maximum of 5 cm/s. Except at the crests, there is very good agreement between the simulated and observed standard deviation profile shape. Above the boundary layer (i.e., $z > 6$), the simulated and observed mean and standard deviation of the horizontal velocity are in very good agreement with the velocities differing less than 0.3 cm/s.

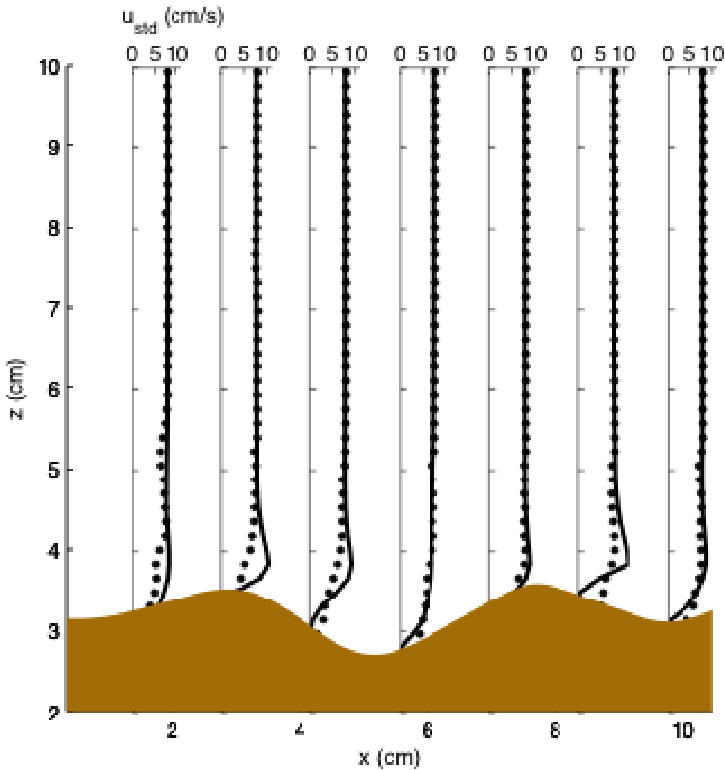


Figure 3: Profiles of the standard deviation of the horizontal velocity from the simulation (lines) and observations (dots) at varying locations above the bed.

4.2 Swirling strength

In complex, three-dimensional, and oscillatory flows, the vortex structures are often difficult to distinguish from the vorticity due to the boundary-generated

shear. The swirling strength, λ_{ci} , is used to identify the coherent closed rotational vortex structures excluding the interference from boundary-generated shear (fig. 4). The swirling strength is calculated as the imaginary part of the complex eigenvalues of the velocity gradient and is zero if the eigenvalues are not complex [13]. The method is effective in determining the location of vortex cores in boundary layer shear flow, but does not identify the rotational direction. The ensemble-averaged swirling strength plotted in Fig. 4 illustrates that the time-varying quantities from the simulation and observations are also in good agreement. The horizontal and vertical positions of the vortices and the timing relative to the wave phase predicted by the model are in good agreement with the observations. The strength of the vortices predicted by the model is only slightly greater than the observations. The observations show less coherent vortex structures and are noisier than the simulation.

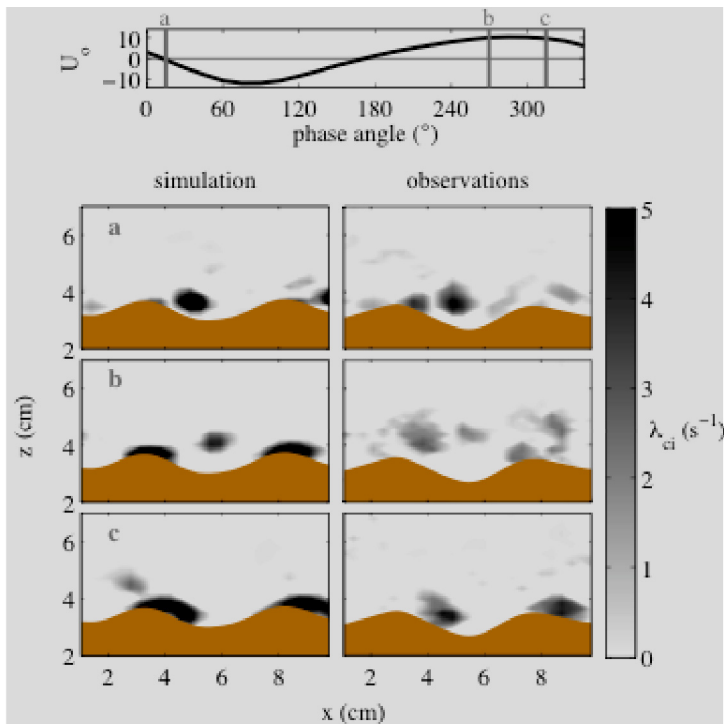


Figure 4: Ensemble-averaged simulated and observed swirling strength, λ_{ci} (s^{-1}), at three phase locations of a wave. Flow is initially directed to the left. Darker areas indicate coherent vortex structures. A time-average of the simulated and observed bed profile is plotted for reference.

5 Discussion

Coherent vortex structures in bottom boundary layer flow over rippled beds have been found to play a significant role in erosion and deposition of sediment on the seafloor. Therefore, a numerical model examining the dynamics of bottom boundary layer flow must accurately predict the temporally and spatially varying velocity fields. While differences in the magnitude of the velocity and swirling strength exist, the simulated vortex location, size and shape agreed remarkably well with the observed vortex structures. The noise associated with making measurements in a laboratory forces the need to smooth the data to remove any outliers. Data smoothing damps out the closed streamline paths of the observed flow measurements, decreasing the strength of the coherent vortices. Typically only very strong circulation events are recorded in situ [14]. In addition, large light reflections at the fluid-sediment interface result in a decreased peak correlation and a lower confidence in the velocity estimates near the bed. The inherent ability of the model to calculate velocities with equal resolution everywhere, even in the highly concentrated layer of moving sediment at the bed would account for some of the differences between the simulated and observed velocity.

6 Conclusions

The turbulent, three-dimensional nature of the wave bottom boundary layer forces the need for three-dimensional, time-dependent simulations in order to fully capture the physics of the flow over ripples. While two-dimensional models are typically less computationally expensive and generally require less storage and processing, they must compensate for their deficiencies in the physics by introducing non-physical terms. Our three-dimensional mixture model has been validated with laboratory data and provides an unprecedented level of detail about sand ripple dynamics that exceeds field and laboratory technologies. Future work will examine the complex, three-dimensionality of the turbulent bottom boundary layer flow over rippled beds.

References

- [1] Blondeaux, P. and Vittori, G., Vorticity dynamics in an oscillatory flow over a rippled bed, *Journal of Fluid Mechanics*, 226, pp. 257-289, 1991.
- [2] Scandura, P., Vittori, G., and Blondeaux, P., Three-dimensional oscillatory flow over steep ripples, *Journal of Fluid Mechanics*, 412, pp. 355-378, 2000.
- [3] Barr, B. C., Slinn, D. N., Pierro, T., and Winters, K. B., Numerical simulation of turbulent, oscillatory flow over sand ripples, *Journal of Geophysical Research*, 109(C9), pp. 1-19, 2004.
- [4] Chang, Y. S. and Scotti, A., Entrainment and suspension of sediments into a turbulent flow over ripples, *Journal of Turbulence*, 4, 2003.



- [5] Zedler, E. A. and Street, R. L., Sediment transport over ripples in oscillatory flow, *Journal of Hydraulic Engineering*, 132(2), pp. 180-193, 2006.
- [6] Rodriguez Abudo, S. and Foster, D.L., Characterization of the wave bottom boundary layer over movable rippled beds, *Eos Trans. AGU, Ocean Sci. Meet. Suppl.*, Abstract PO21B-05, 2010.
- [7] Penko, A. M., Slinn, D. N., and Calantoni, J., Model for mixture theory simulation of vortex sand ripple dynamics, *Journal of Waterway Port Coastal and Ocean Engineering- ASCE*, in press.
- [8] Eilers, H., The viscosity of the emulsion of highly viscous substances as function of concentration, *Kolloid-Zeitschrift*, 97(3), pp. 313-321, 1941.
- [9] Einstein, A., Eine neue Bestimmung der Moleküldimensionen (German) [A new determination of molecular dimensions], *Annalen der Physik*, 19, pp. 289-306, 1906.
- [10] Nir, A. and Acrivos, A., Sedimentation and sediment flow on inclined surfaces, *Journal of Fluid Mechanics*, 212, pp. 139-153, 1990.
- [11] Richardson, J. F. and Zaki, W. N., Sedimentation and fluidisation: part 1, *Transactions of the Institution of Chemical Engineers*, 32, pp. 35-53, 1954.
- [12] Leighton, D. and Acrivos, A., Viscous resuspension, *Chemical Engineering Science*, 41(6), pp. 1377-1384, 1986.
- [13] Zhou, J., Adrian, R. J., Balachandar, S. and Kendall, T. M., Mechanisms for generating coherent packets of hairpin vortices in channel flow. *Journal of Fluid Mechanics*, 387, pp. 353–396, 1999.
- [14] Nichols, C. S. and Foster, D. L., Full-scale observations of wave-induced vortex generation over a rippled bed, *Journal of Geophysical Research*, 112(C10), 2007.

